

Vesic



gao@phy.duke.edu
11/14/2003 12:20 PM

To: lsc-requests@notes.duke.edu
Subject: Please fill LSC/DOSS request for...

This data was submitted on: Friday, November 14, 2003 at 12:20:22

ID NUMBER:
0297689

NAME:
Haiyan Gao

PHONE:
660-2622

CLIENT_EMAIL:
gao@phy.duke.edu

STATUS:
Faculty

CALL NUMBER:

TITLE:
Journal of low temperature physics

VOL:
76

YEAR:
1989

NUMBER:

PAGES:
435

AUTHOR:

TITLE OF ARTICLE:

NO LONGER:

DELIVER_TO:
Vesic Library

STATUS:
Faculty

NOTES:
Prefer Email delivery if possible by the end of the day.

Do1803486U

Liquid ^4He as a Cryogenic Coating for Gaseous Spin Polarized ^3He

M. Himbert and J. Dupont-Roc

Laboratoire de Spectroscopie Hertzienne de l'Ecole Normale Supérieure,* Paris, France

(Received November 25, 1988, revised February 28, 1989)

Nuclear spin polarization can be produced by optical pumping of ^3He gas in sealed samples at a temperature below 1 K. The wall relaxation can be minimized by covering the container walls with a ^4He film, and relaxation times T_1 longer than 1000 sec have been observed. A study of the residual relaxation is reported here. Spin relaxation appears to take place near the helium-substrate boundary. This situation is characterized by an "adsorption" energy very different from the known binding energies of ^3He quasiparticles on and in bulk liquid ^4He . Models are presented which reproduce the observed T_1 variations on temperature and on other experimental parameters.

1. INTRODUCTION

In a previous publication,¹ we have reported that it is possible to obtain by optical pumping a nuclear polarization in ^3He gas, using ^4He as a coating to prevent wall relaxation.

The technique of cryogenic coatings have been used for more than ten years to diminish the sticking time of atoms on walls. The coatings are obtained by condensing diamagnetic materials on the walls of the container at low temperature. To conserve ^3He nuclear polarization out of equilibrium, various atomic or molecular gases have been successfully tried as coating materials.²⁻⁵ To be effective at low temperature, a coating must bind ^3He atoms as weakly as possible. The best one used so far is solid molecular hydrogen, which is characterized by a binding energy of the order of 12 K.⁴ It is not useful at temperatures lower than about 2 K.

Liquid ^4He interacts less strongly with ^3He than does solid hydrogen. ^3He has a bound state at the free surface with an energy of -5 K .⁶ It can also enter the bulk liquid, with an energy of -2.78 K .⁷ (^3He energies are

*Laboratoire associé au Centre National de la Recherche Scientifique et à l'Université Paris VI.

taken to be zero in vacuum, far from the liquid). Hence ^4He film was a natural choice for conserving ^3He polarization below 2 K.

In fact, such films have already been used in the experiments on polarized atomic hydrogen to prevent wall recombination.⁸⁻¹⁰ It is also known that small amounts of ^4He can reduce the magnetic coupling between liquid ^3He and magnetic impurity in walls^{11,12} and that polarized ^3He in dilute solution in ^4He exhibits long relaxation times.¹³ Hence the success reported in (Ref. 1) was not unexpected. Nevertheless, in connection with the developing experiments on polarized ^3He ,¹⁴⁻¹⁶ it is interesting to investigate the limitations of such a coating, and, for that purpose, to get a better understanding of its behavior. Spin relaxation could also be a new way to study ^3He atoms in ^4He films, a problem of interest in connection with the various investigations on ^3He - ^4He mixture films.¹⁷⁻²⁰ This is the subject of this article. It is worth mentioning that parallel and complementary studies were conducted at Sussex University. The corresponding results are reported in Ref. 21 and 22.

2. EXPERIMENTAL SET-UP AND PROCEDURES

The experimental arrangement is shown in Fig. 1. The ^3He atoms are contained in sealed pyrex spherical bulbs, 3 cm in diameter, with densities ranging from 10^{16} to 10^{17} cm^{-3} . The cells (ce) are thermalized by a superfluid helium bath (ba) to a ^3He refrigerator (frig). The temperature can be varied from 0.5 K up to 2 K. Thermalization at 4.2 K can also be achieved. The 2^3S_1 metastable states necessary to the optical pumping process are produced by a weak 10 MHz rf discharge induced by external electrodes (el) and dissipating a power of a few milliwatts. The light beam (L) originates from a single mode laser developed by M. Leduc.²³ A typical power of 60 mW on the so-called C_9 hyperfine transition²⁴ produces a nuclear polarization of the order of three percent. An NMR detection system was set up to detect the nuclear polarization after the discharge has been turned off. It is a crossed coils system [(ic) for inducing coils, (rc) for receiving ones] operating at a frequency of 44 kHz, which corresponds to the Larmor frequency in a field of 1.4×10^{-3} Tesla produced by the main coils (co). With a 30 msec time constant, the noise in the detection channel is equivalent to the signal produced by 10^{14} coherently precessing ^3He spins.

The magnitude of the longitudinal polarization is monitored by a fast adiabatic passage technique:²⁵ the magnetic field is swept through resonance in presence of an homogeneous rf field, a few 10^{-7} Tesla in amplitude, in a time short with respect to T_2 , but long compared to the period of precession around the effective field in the rotating frame. Under these conditions, the magnetic moments follow the effective field, and the voltage amplitude

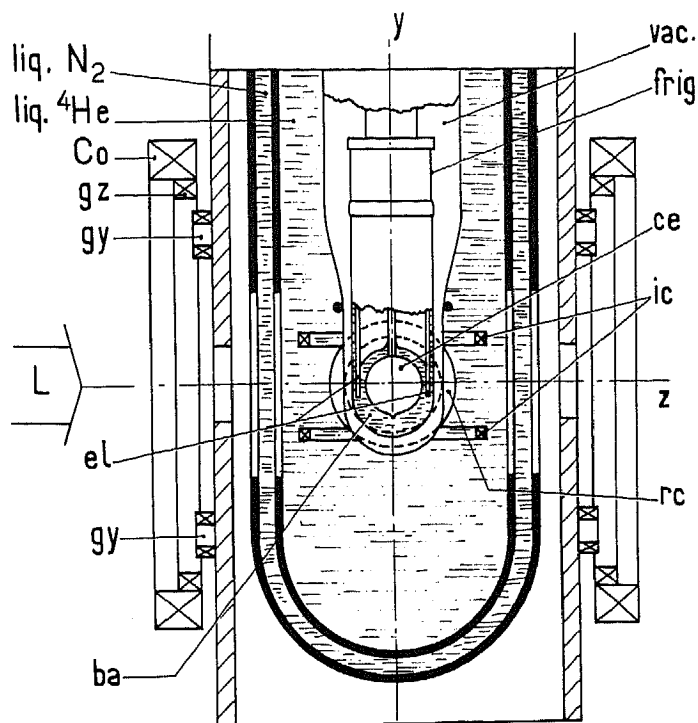


Fig. 1. Sketch of the experimental set-up. Symbols are defined in the text.

induced in the receiving coils by the precessing spins gives a measurement of the total magnetization. The calibration of the pair of receiving coils was carefully calculated, and checked by inducing a resonant oscillating field in a small, one-turn coil in place of the cell. The magnitude of the polarization achieved by optical pumping was measured in that way. The same detection process was used to monitor the decay of the polarization due to wall relaxation. The longitudinal polarization was measured three or four times during the decay, and the longitudinal relaxation time T_1 was extracted through an exponential fit. Note that the fast adiabatic passage technique requires a long transverse time T_2 . This was achieved by a careful elimination of magnetic and superconducting materials from the vicinity of the cell. Gradient coils (g_z , g_y) were also used to compensate the residual static gradient. The field homogeneity over the entire cell was typically better than 10^{-7} Tesla. The longitudinal relaxation rate corresponding to this field inhomogeneity²⁶ is of the order of 10^{-7} sec^{-1} , well below the observed wall relaxation rate. Also, the intrinsic relaxation time due to two body collisions in the gas²⁷ is completely negligible at the densities considered here.

3. ^4He AS A CRYOGENIC COATING

The fact that ^4He indeed behaves as a cryogenic coating is illustrated in Fig. 2. T_1 is plotted (logarithmic scale) versus the inverse temperature $1/T$ for T ranging from 4.2 K to 0.6 K, for a cell * filled at room temperature with ^3He , ^4He , and H_2 (respective densities $3.3 \times 10^{17} \text{ cm}^{-3}$, $6.5 \times 10^{16} \text{ cm}^{-3}$, $4.8 \times 10^{16} \text{ cm}^{-3}$). For temperatures higher than 2 K ($1/T = 0.5 \text{ K}^{-1}$), the wall is effectively bare solid hydrogen, and T_1 is quite long. In T_1 decreases as $1/T$ increases, because of the growing number of ^3He atoms adsorbed on the wall. The slope of the curve is twice the adsorption energy $E_{^3\text{He}/\text{H}_2}$ of ^3He on solid hydrogen as expected from previous studies.⁴ In T_1 reaches a minimum for $1/T \approx 0.8$ and then starts to increase when the temperature is lowered reaching a value of 1000 sec at $1/T \approx 1.4$. Beyond $1/T \approx 1.5$, T_1 decreases again, but with a slope much weaker than in the high-temperature region. This behavior suggests strongly that, as soon as helium begins to cover the solid hydrogen coating, ^3He is expelled from the vicinity of the wall, and the energy characterizing the binding of ^3He in this region is much weaker than on bare solid hydrogen. Thus, liquid ^4He is a fairly effective cryogenic coating preventing strong wall relaxation for temperatures as low as 0.5 K.

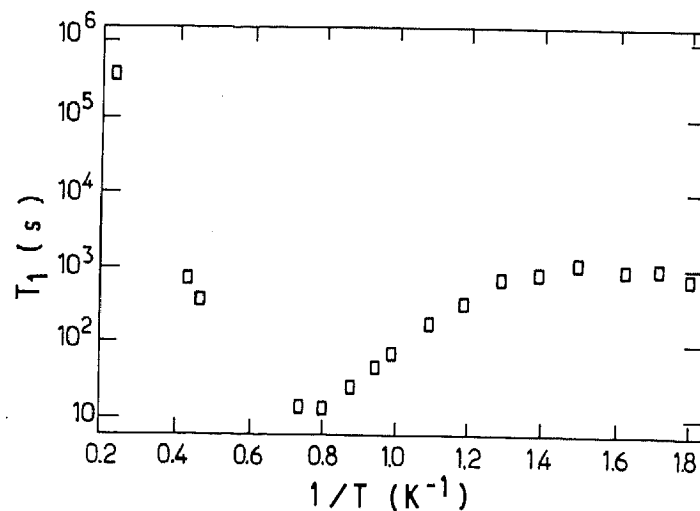


Fig. 2. Longitudinal relaxation time T_1 (logarithmic scale) versus the inverse temperature between 4.2 K and 0.5 K for a particular cell. Lower temperatures are on the right part of the figure.

*This cell was prepared at Sussex University by C. Lusher and M. Richards (see Refs. 21 and 22). It is 2 cm in diameter contrary to all other tested cells (3 cm).

However questions remain concerning the mechanism by which a ^4He film prevents relaxation of ^3He . For solid hydrogen coating, the energy required for inserting a helium atom is believed to be positive and large, and only ^3He atoms adsorbed on the surface play a significant role in the wall relaxation. It is well known, on the other hand, that ^3He dissolves in ^4He at low concentration²⁸ (its chemical potential is negative). Hence questions arise. Where are the relaxing atoms? On the surface or inside the ^4He film? Is it possible to explain the variation of $\ln T_1$ with $1/T$? What is the significance of the slope of the curve on the low-temperature side? And finally, is it possible to improve significantly the relaxation times at low temperatures? To clarify some of these questions, we have performed various experiments, varying the coating thicknesses, the temperature, the ^3He density. The results are reported here. We have also built up some simple models to explain the observed phenomena.

4. VARYING THE THICKNESSES

Varying the thickness of the hydrogen coating or that of the ^4He film is a simple means to test various hypothesis about the relaxation mechanism. Of course, only the total quantity of gas put in the cell can be controlled easily, and we have to rely on available knowledge to estimate the real thicknesses. To quantify each situation, the total amount of coating materials will be given as a thickness e_0 (e_{04} for ^4He , e_{02} for hydrogen) expressed in geometrical layers (G. layers). It is calculated under the following assumptions: (i) the material is supposed to be condensed as a uniform film on the inner surface of the cell; (ii) the area of this surface is taken as the geometrical (i.e., macroscopic) area of the cell; (iii) the density of the condensed material is approximated by the bulk density.

In fact, e_0 represents an upper bound for the actual thickness at a given point in the cell, either because the effective area of the inner surface may be larger than the geometrical one, or because of an incomplete or non uniform condensation.

4.1. Changing the ^4He Thickness

This can be achieved in two ways. One can first vary the temperature of a given cell around the temperature T_0 for which the ^4He gas density becomes saturated. Numerous experiments on helium films (see, for instance, Ref. 29) have demonstrated that the first layers condense for T higher than T_0 . In that regime, one can compute an approximate thickness e_4 from the Frenkel-Halsey-Hill (FHH) law:³⁰

$$-\frac{C_3}{e_4^3} = kT \ln \left(\frac{d_4}{d_{s,4}(T)} \right) \quad (1)$$

where d_4 is the filling density, $d_{s4}(T)$ is the saturating density at temperature T , and C_3 is the appropriate Van der Waals constant. When T is lowered well below T_0 , a large proportion of ^4He atoms is condensed. The ^4He density in the gaseous phase is then very close to $d_{s4}(T)$ and becomes negligible at sufficiently low temperature. To compute the film thickness around T_0 , one has to take into account the depletion of the gas phase in formula (1), replacing d_4 by $d_4 - n_{\text{liq}}(e_4 A / V)$, where n_{liq} is the liquid density, A the film area, and V the cell volume, and then solve for e_4 .

Figure 3 gives the variation of T_1 when T is lowered. For that cell, T_0 is equal to 0.75 K (or $1/T_0 = 1.33 \text{ K}^{-1}$). It coincides with the abscissa of the shoulder of the experimental curve. Decreasing T from T_0 down to 0.5 K makes T_1 decrease weakly, by only a factor 1.3. But in the same temperature range, the quantity of condensed ^4He varies from 5 G. layers to 36 G. layers. Hence T_1 does not appear to be very sensitive to the thickening of the film. However, since parameters other than e_4 also vary, these data do not allow a more precise conclusion.

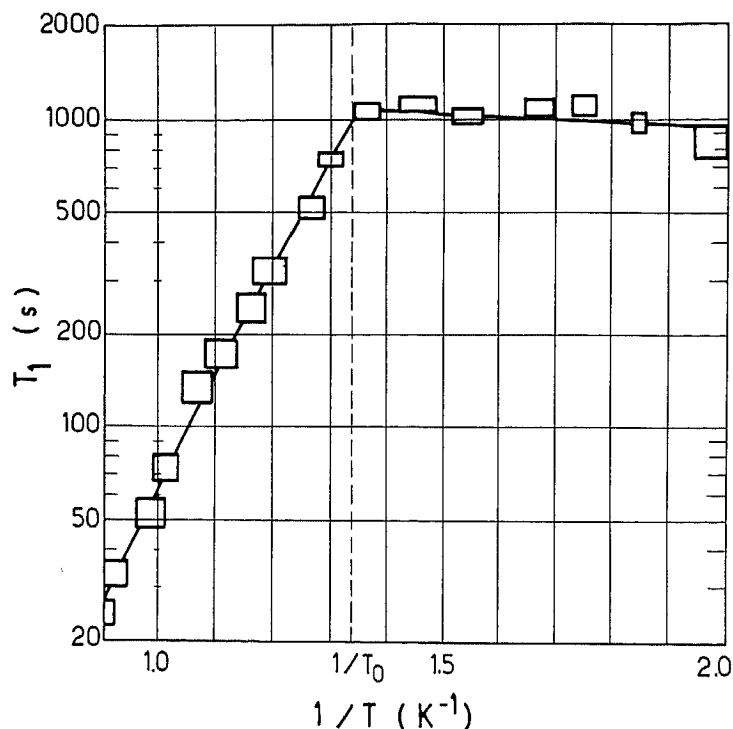


Fig. 3. Longitudinal relaxation time T_1 (logarithmic scale) versus the inverse temperature. T_0 is the condensation temperature for ^4He in the cell. Solid curve is the theoretical fit obtained according to the model of section 4.

Thus, we studied also, at the same temperature, cells with different ^4He content. The temperature was chosen as low as possible (around 0.53 K), that essentially all of ^4He was condensed in each case. More precisely, the quantity of ^4He varied from 6 G. layers to more than 60 G. layers, corresponding to filling densities ranging from 10^{16} cm^{-3} to 10^{17} cm^{-3} .

The results are shown in Fig. 4. At 0.53 K, the ^4He saturated vapour density is about 10^{15} cm^{-3} and for all the studied cells, more than 90% of the ^4He was condensed. This was checked by monitoring the diffusion coefficient of ^3He in the gaseous phase,³¹ which indeed undergoes a variation when the temperature is lowered according to the ^4He vapor density. Hence within the experimental uncertainty and reproducibility, T_1 is independent of the quantity of ^4He , e_{04} . More precisely the shape of the variations of T_1 versus $1/T$ are the same for all the cells and similar to that of Fig. 3. For increasing quantity of ^4He , the left part of the curve is shifted left, according to the higher value of T_0 . But the low-temperature parts of the curves fall roughly on a same straight line with a weak negative slope. Hence, one can conclude that the thickening of the ^4He film in excess of

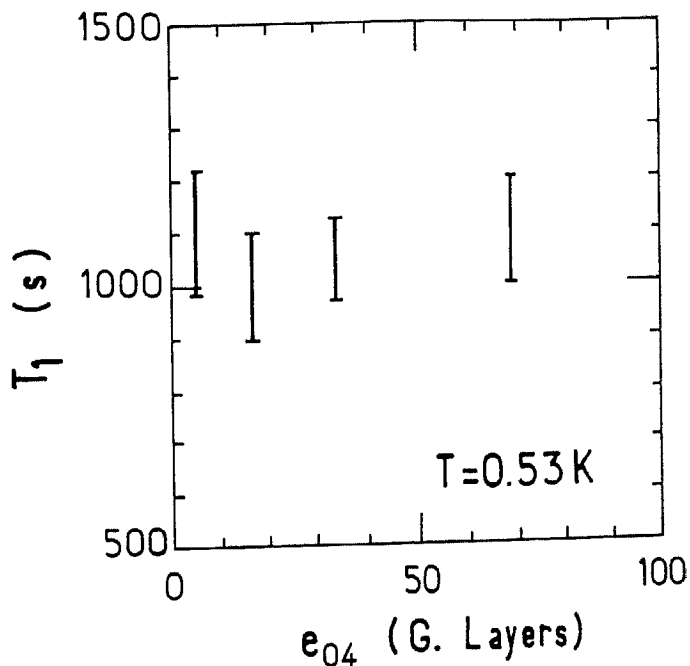


Fig. 4. Values of T_1 at $1/T = 1.89\text{ K}^{-1}$ as function of the ^4He quantity e_{04} in the cell.

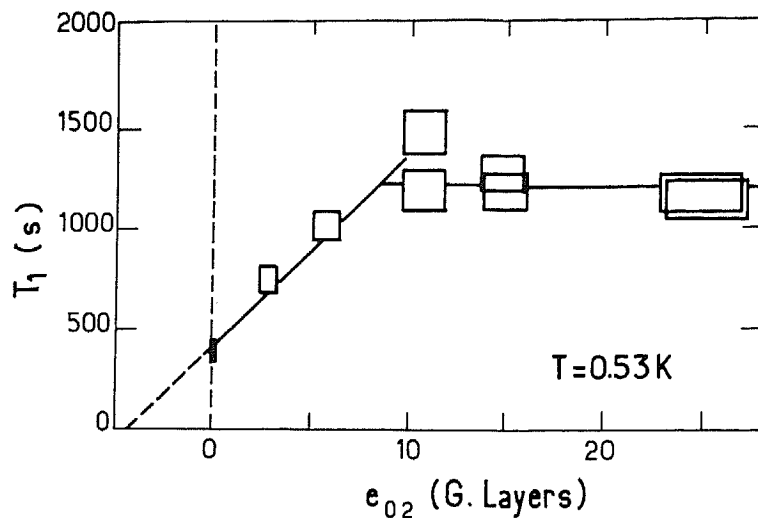


Fig. 5. Values of T_1 at $1/T = 1.89 \text{ K}^{-1}$ as function of the H_2 quantity e_{02} in the cell.

six layers (or possibly less if an effective area larger than the geometrical one is taken into account) does not influence the wall relaxation.

4.2. Changing the H_2 Thickness

Cells with identical ^3He and ^4He content, but different H_2 filling densities, were also studied. The quantity of hydrogen was varied from 0 to 30 G. layers. This does not mean that the film was thickened up to that value. It is known that solid rare gas films grow in a uniform manner up to a thickness depending on the substrate, bulk solid forming somewhere thereafter.³² Assuming that solid hydrogen on glass behaves in that way, and following the model presented by Krim *et al.*³³, one can estimate the maximum thickness to be of the order of 3 or 4 layers.³⁴ But the microscopic arrangement of the glass surface is likely to affect this value.

It was found that the hydrogen quantity does have an influence on T_1 . For different cells, the curves $\ln T_1$ versus $1/T$ are shifted vertically, indicating that the hydrogen thickness acts as a scale factor on T_1 . To show this we plotted, in Fig. 5, T_1 at 0.53 K on a linear scale versus e_{02} . T_1 increases roughly linearly with e_{02} from 0 to 10 G. layers, and then becomes constant.

4.3. Discussion

The most natural explanation for this behavior is to assume that the hydrogen thickness increases with the quantity of hydrogen initially put in the cell, at least up to 10 G. layers, and that the hydrogen coating is situated between the relaxing ^3He atoms and the sources of the relaxing magnetic

field. Under this hypothesis, it appears that this field varies significantly on distances of the order of a few atomic layers, and consequently that its origin is not far below the hydrogen coating. Conversely, since the ^4He thickness has no influence on the relaxation, we are led to conclude that the relaxing atoms are inside the layers of the ^4He film, close to the hydrogen surface (closer than 6 layers). Let us assume for the moment that T_1 could exhibit a linear variation with the distance between the sources of the inhomogeneous magnetic field and the relaxing ^3He atoms. In the next paragraph, we will discuss a model which indeed shows such a behavior. Under this hypothesis, the leveling of T_1 for e_{02} larger than 10 G. layers could be associated with the limited growth of the hydrogen film described in the preceding section. An effective geometrical area ratio of 2.5 would reduce the 10 G. layers to 4 layers, which is not unrealistic. The non-zero intercept on the T_1 axis in Fig. 5 reveals that, even in absence of hydrogen, there is a non-zero distance between the source of relaxation and the ^3He atoms. Keeping the value 2.5 mentioned above for the effective area ratio, we get a minimum distance of about 1.7 G. layers. It would mean that the surface of the glass itself is free from magnetic impurities and that they are located deeper in the bulk. It could be also that the ^3He atoms do not enter in the first one or two ^4He layers close to the substrate. Both features may be present at the same time. Although we cannot give direct evidence that this indeed occurs in the cells, none of these phenomena is unlikely: it is known that the surface of glasses is often chemically different from the bulk,^{35,36} and that the ^3He atoms are excluded from the vicinity of the substrate in ^3He - ^4He films.^{11,12,20}

Before discussing the linear variation of T_1 with e_{02} , it should be mentioned that a different explanation could be proposed for the fact that T_1 is independent of e_4 at low temperature. If the growth of the ^4He film was limited to a value lower than the minimum value of 6 determined experimentally, the preceding discussion localizing the relaxing atoms close to the wall in the ^4He film would be invalidated. Atoms at the free surface of the film would be affected in the same way by the magnetic field of wall with little or much ^4He in the cell. Observation of such a limited growth of ^4He films has been claimed on some metallic surfaces.³⁴ This is unlikely to be pertinent for our case. The maximum thickness quoted in Ref. 33 and 34 is about 8 to 10 layers, larger than our 6 G. layers. Indeed, the growth of ^4He films on solid hydrogen has been observed layer by layer up to 10 layers.²⁹ Hence the fact that T_1 at low temperature does not vary when e_4 changes from 6 to 10 layers rules out the limited growth explanation.

4.4. Linear Variation of T_1 with e_2

Wall relaxation of polarized gases have been studied for a long time.^{4,37,38} Recently, Berlinsky *et al.* published a theoretical quantum model

describing the spin relaxation of atomic hydrogen near a wall containing magnetic impurities.³⁹ We consider here a model in which the relaxing atoms are adsorbed on a surface with statistically uniform properties. The surface is approximated locally by a plane. Its orientation is isotropically distributed over the spherical cell. The atoms move on the surface either by diffusion or freely for a duration τ given by a Poisson law $(1/\tau_s) \exp(-\tau/\tau_s)$, τ_s being the mean dwell time. This motion is treated classically. We ignore the relaxation processes that could occur when the atoms are approaching or leaving the wall.

The relaxing magnetic field \mathbf{B}_1 is assumed to be produced by fixed dipoles situated in the glass at a distance e_2 below the plane where the atoms move. We consider two coordinate systems: the laboratory axis XYZ , Z being along the direction of the static field \mathbf{B}_0 , and a local frame on the glass surface for which the glass surface is taken as the origin for the z -coordinate, x and y being the two coordinates in the plane parallel to the surface. The relaxation rate of the adsorbed phase is given by²⁵

$$\left(\frac{1}{T_1}\right)_a = 2\gamma^2 \operatorname{Re} \left\{ \int_0^\infty d\tau e^{i\omega_0\tau} \iint dx dy P(x, y; \tau) \sum_i \overline{B_{1i}(0, 0, e_2) B_{1i}(x, y, e_2)} \right\} \quad (2)$$

The sum over i is taken for the two components X and Y of \mathbf{B}_1 , $\omega_0/2\pi$ is the Larmor frequency, and γ the gyromagnetic ratio of the spin. The distribution $P(x, y; \tau)$ is the probability that an atom starting from the origin ($x = y = 0$) at $\tau = 0$ is at the point x, y at time τ . The average bar on $B_{1i}(0, 0, e_2) B_{1i}(x, y, e_2)$ accounts for the distribution of magnetic impurities in the wall and for the average over the orientation of the surface with respect to \mathbf{B}_0 .

Introducing the Fourier transforms

$$\mathcal{E}_{ij}(\mathbf{q}, e_2) = \frac{1}{2\pi} \iint dx dy \overline{B_{1i}(0, 0, e_2) B_{1j}(x, y, e_2)} \times \exp[-i(q_x x + q_y y)] \quad (3a)$$

$$\mathcal{P}(\mathbf{q}, \omega) = \frac{1}{2\pi} \iint dx dy \int_0^\infty d\tau P(x, y; \tau) e^{i\omega\tau} \times \exp[-i(q_x x + q_y y)] \quad (3b)$$

the relaxation rate can be written in the form

$$\left(\frac{1}{T_1}\right)_a = \gamma^2 \int d^2 q \left[\mathcal{P}^*(\mathbf{q}, \omega_0) \sum_i \mathcal{E}_{ii}(\mathbf{q}, e_2) + \text{c.c.} \right] \quad (4)$$

It is easy to show⁴⁰ that under the hypothesis of randomly distributed paramagnetic sources, the correlation function for the magnetic field is an exponential function of e_2

$$\sum_i \mathcal{G}_{ii}(\mathbf{q}, e_2) \propto q \exp(-2qe_2) \quad (5)$$

For a diffusive motion, interrupted by desorption, the Green function $\mathcal{P}(\mathbf{q}, \omega_0)$ is

$$\mathcal{P}(\mathbf{q}, \omega_0) \propto \frac{1}{Dq^2 + (1/\tau_s) + i\omega_0} \quad (6)$$

Substituting (5) and (6) into (4) gives

$$\left(\frac{1}{T_1}\right)_a \propto \int_0^\infty q dq \left(\frac{q e^{-2qe_2}}{Dq^2 + 1/\tau_s + i\omega_0} + \text{c.c.} \right) \quad (7)$$

Depending on the relative magnitude of D/e_2^2 , $1/\tau_s$, and ω_0 , formula (7) gives rise to various dependences of $(1/T_1)_a$ on e_2 .

(i) $D/e_2^2 \gg 1/\tau_s, \omega_0$. This corresponds to the low-field limit, with long adsorption times. Integration of (7) gives immediately

$$\left(\frac{1}{T_1}\right)_a \propto \frac{1}{e_2} \quad (8)$$

Hence, a linear variation of $(T_1)_a$ with e_2 is found in that case. According to the proportionality between T_1 and $(T_1)_a$ (see Sec. 5.1), T_1 varies also linearly with e_2 , as found experimentally (see Sec. 4.2).

(ii) $1/\tau_s$ or $\omega_0 \gg D/e_2^2$. This is the high-field (or short-dwell time) limit. Formula (7) gives

$$\left(\frac{1}{T_1}\right)_a \propto \left(\frac{1}{e_2}\right)^3 \quad (9)$$

At last, note that for the case of atoms moving freely on the surface, with a Boltzmannian distribution of velocities v , formula (6) should be replaced by

$$\mathcal{P}(\mathbf{q}, \omega_0) \propto \exp\left(-\frac{\omega_0^2}{wq^2v^2}\right) \quad (10)$$

giving the results discussed in Ref. 39.

Thus various behaviours as function of the thickness, including a linear variation of T_1 with e_2 , can be produced under simple and reasonable assumptions concerning the motion of the atoms and the sources of the magnetic field producing the relaxation.

4.5. Conclusion

To summarize, the experimental results concerning the thicknesses can be well explained by supposing that wall relaxation acts mainly on ^3He

atoms located inside the ^4He film close to the interface between solid hydrogen and liquid helium. It remains now to examine if the measured temperature dependence of T_1 supports such an hypothesis.

5. VARIATIONS OF T_1 WITH TEMPERATURE

This temperature dependence has the shape shown in Fig. 3. A strong rise of T_1 when $1/T$ is increased up to the condensation point, followed by a slow decrease. Both parts of the curve are approximately linear. Variations of relaxation rates with temperature usually give information on the binding energy of the observed atoms on the walls.^{4,37,38} In the present case, one can expect them to be related to the binding energy of ^3He atoms in the ^4He film near the substrate. Since the ^4He film also changes with temperature, the variation of this energy with temperature has to be taken into account. In fact, little information is available on the microscopic behavior of a ^3He atom in such conditions.^{18,20} We will propose here a simple model with few parameters to reproduce the temperature dependence of T_1 .

5.1. Description of the model

We assume that the spin polarization is destroyed when the ^3He atoms reach, inside the ^4He film, a region which is closed to the hydrogen coating. This region is supposed to be characterized by a unique potential energy E_3 . Such an hypothesis would make no sense for a continuous description of ^4He , since E_3 would vary continuously with the distance to the boundary with solid hydrogen. However, it is known that close to a substrate, liquid helium is significantly structured in layers.²⁹ The situation of a ^3He atom is likely to be different from one layer to the other, at least for the first ones. Hence one can think of E_3 as the energy of ^3He in a state localized in one of these first layers.

Then the relaxation rate $1/T_1$ of the sample is proportional to the fraction N_a/N of atoms in the states defined above, which is obtained by expressing the equilibrium with the gas phase. Since these states have a finite extension in the direction perpendicular to the wall, we will approximate their density by that of a two-dimensional gas, so that finally

$$\frac{1}{T_1} = \left(\frac{1}{T_1}\right)_a \frac{N_a}{N} \quad (11a)$$

$$\frac{N_a}{N} = \lambda_3(T) \frac{A}{V} \exp\left(-\frac{E_3}{kT}\right) \quad (11b)$$

$(1/T_1)_a$ depends on microscopic parameters, in particular transport coefficients of ^3He in the region of interest. V is the volume of the sample, A the area of the relaxing region, and $\lambda_3(T)$ is the thermal de Broglie wavelength associated with the ^3He quasiparticles. This last factor could also include renormalization factors, such as the ratio of the effective mass of ^3He in ^4He to the free mass.

We assume that the energy E_3 is a linear function of the chemical potential μ_4 of ^4He in the cell

$$E_3 = E_3^0 + (1 + \alpha)[\mu_4(T) - L_4] \quad (12)$$

where L_4 is the chemical potential of liquid ^4He at zero pressure and temperature.

Such a linear relation exists for the energy of the ^3He quasiparticle in bulk $^4\text{He}^*$ when μ_4 is not far from L_4 . α is then close to 0.25 and represents the relative excess volume of a ^3He atom in liquid ^4He (^3He is lighter than ^4He , and its zero point motion has a larger amplitude), and E_3^0 is the binding energy of ^3He in bulk helium four, $E_3^0 = E_3^b = -2.78$ K. The relation (12) can be used for wider variations of μ_4 , including the solidification transition, but gives then only a good order of magnitude.

We generalize here the relation (12) to an inhomogeneous situation.[†] In the vicinity of the hydrogen substrate, liquid ^4He is compressed by the Van der Waals attraction due to solid hydrogen. Hence the relation between the local binding energy of ^3He and the chemical potential of ^4He inside the cell will correspond to values of the parameters E_3^0 and α different from the above quoted bulk values.

5.2. Predicted Variations with Temperature

Postulating that $(1/T_1)_a$ varies like the inverse of a diffusion coefficient, i.e., as $1/\sqrt{T}$, and putting together (11a), (11b), and (12) leads to the expression

$$\ln(T_1) = C + \ln(T) + \frac{1}{kT} [E_3^0 + (1 + \alpha)(\mu_4(T) - L_4)] \quad (13)$$

where C is a constant term. The variation with T of the chemical potential μ_4 of ^4He in the cell can be determined as follows. If one first neglects surface effects, μ_4 is equal to L_4 below the condensation temperature T_0 and, above T_0 , μ_4 is the chemical potential of a ^4He gas at the filling density.

*This can be readily obtained from Table I of Ref. 7. It has been examined on a wider range of pressure in ref. 40.

†An approach to this situation could be to consider separately the first layer of helium onto the substrate as a bidimensional system. A relation of the type (12) can be obtained with such a model.⁴⁰

This chemical potential can be approximated by that of a perfect gas because of the low density and temperature.

$$\mu_4 = L_4, \quad \text{for } T < T_0$$

$$\mu_4 = kT \ln[n_4 \lambda_4^3(T)], \quad \text{for } T > T_0$$

The transition between these two regimes is in fact smoothed by the Van der Waals attraction which is responsible for the pre-condensation. Taking a reasonable model for the potential of hydrogen coating onto ^4He ,* one gets, in the particular case already discussed in Sec. 3, the variation shown in Fig. 6.⁴² Its variation is similar to that of the variation of T_1 in Fig. 3. Hence $\mu_4(T)$ is the key parameter governing the temperature variation of T_1 .

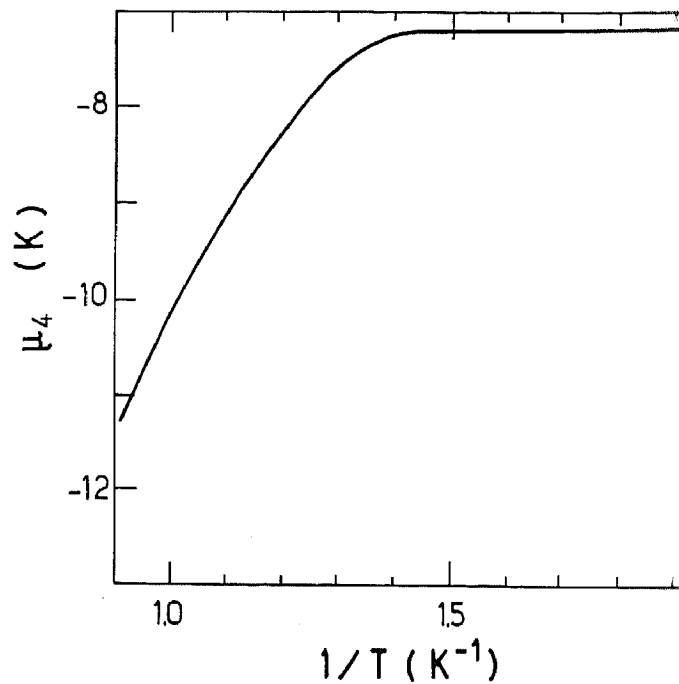


Fig. 6. Chemical potential μ_4 of ^4He in the cell giving the T_1 values in Fig. 3, versus the inverse temperature.

*It is a simple Frenkel-Halsey-Hill approximation θ/z^3 with $\theta = 7 \text{ K} \times (1 \text{ \AA})^3$, $z = 3.58 \text{ \AA}$.

5.3. Comparison with the Experimental Results

We computed $\mu_4(T)$ for various cells and tried to fit the experimental variation of T_1 with $1/T$ using the expression (13), C , E_3^0 , α being taken as adjustable parameters. Figure 7 shows fits for three particular cases. Fair agreement is easily obtained. The fit is not very sensitive to the value of α , but it appears that for low ^3He densities $\alpha \approx 0$ is better, whereas $\alpha \approx 0.25$ is more appropriate for $n_3 \geq 10^{17} \text{ cm}^{-3}$.

Figure 8 shows the distribution of the values E_3^0 found for thirty-one different cells. Whereas the binding energy of ^3He is -2.78 K in the bulk ^4He and -5 K on the bulk surface, all optimal measured values for E_3^0 are larger than -2.2 K . A first group, around $E_3^0 = 0.3$ with a dispersion of 0.4 K ,

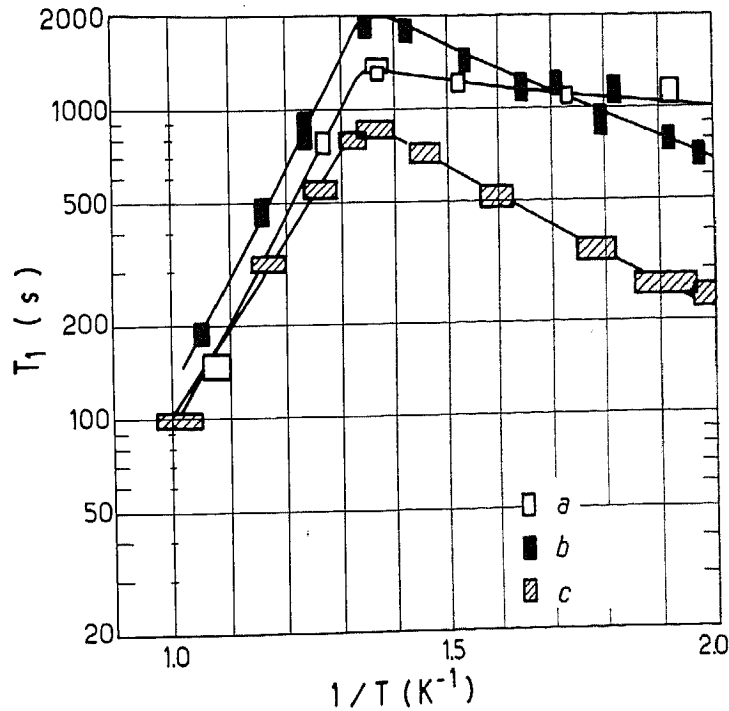


Fig. 7. Longitudinal relaxation time T_1 (logarithmic scale) versus the inverse temperature, for three particular cells with the following ^3He filling densities (n_3 , cm^{-3}), and the following coating maximum thicknesses for ^4He (e_{04} , G. layers) and H_2 (e_{02} , G. layers). a: $n_3 = 6, 2 \times 10^{16}$, $e_{04} = 37$, $e_{02} = 27$. b: $n_3 = 2, 6 \times 10^{17}$, $e_{04} = 37$, $e_{02} = 11$. c: $n_3 = 6, 4 \times 10^{16}$, $e_{04} = 37$, $e_{02} = 27$. The fitted curves correspond, according to formula (13), to the following values of the parameters α (dimensionless) and $E_3^0(\text{K})$: a, $\alpha \approx 0.00$, $E_3^0 = +0.1$; b, $\alpha = 0.26$, $E_3^0 = -0.9$; c, $\alpha \approx 0.05$, $E_3^0 = -1.7$.

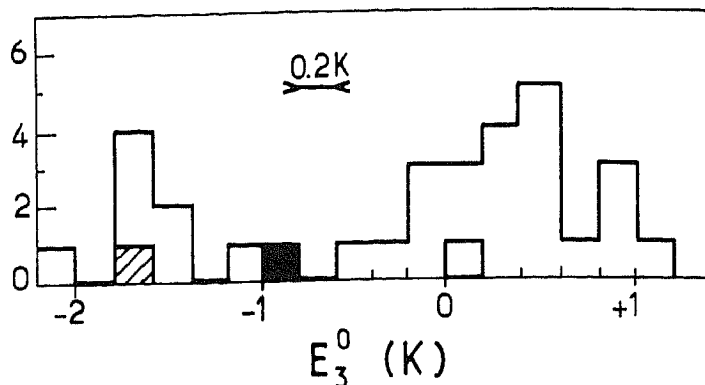


Fig. 8. Distribution of the values of E_3^0 (binding energy of the relaxing atoms) for the tested cells. The particular values corresponding to the three curves reported in Fig. 7 have been specified, using the same symbols as in Fig. 7.

contains the majority of the samples. The fact that this energy is significantly higher than the quoted bulk value indicates that the corresponding ^3He atoms are located in a region where ^4He is compressed, i.e., close to the hydrogen substrate (see for example the Fig. 1b of Ref. 20). A smaller group, around $E_3^0 = -1.7$ K, corresponds to cells with a steeper slope at low temperature. This behavior has been correlated with cells more recently blown from a different batch of pyrex. We have presently no convincing proposal to explain how the nature of the pyrex glass could produce such a change.

It must be kept in mind that, in formula (13), the term $\ln(T)$ could be multiplied by a factor larger than one, depending on the hypothesis made on the motion of the relaxing atoms. This however does not improve the fits, but increases E_3^0 by 0.3 K to 0.4 K. This is of the order of the experimental fluctuations of E_3^0 and does not change the above conclusions.

5.4. Comparison with Results at Higher Field

For one of the cells (the one for which T_1 is reported in Fig. 2), the relaxation time T_1 has also been studied by the Sussex group at higher field ($\omega_0/2\pi = 7.7$ MHz).^{21,22} In the temperature range $0.6 \text{ K}^{-1} < 1/T < 1.6 \text{ K}^{-1}$, the corresponding values of T_1 are substantially longer than those taken in Paris at $\omega_0/2\pi = 45$ kHz. If one attributes this difference to the variation of the spectral density of the relaxing perturbation between these two frequencies, we get a crude estimate for its correlation time τ_c . A simple exponential decay for the correlation function would give a T_1 dependence on ω_0 of the form $[1 + (\omega_0\tau_c)^2]$. With such a model, τ_c is found of the order of $0.1 \mu\text{sec}$ and is constant within a factor two in the temperature range $0.6 \text{ K}^{-1} \leftrightarrow 1.6 \text{ K}^{-1}$. This correlation time is quite long. It is much longer than the

correlation time of liquid helium associated with lengths of the order of a few angströms (10^{-12} sec), and larger than the time of flight of ^3He quasiparticles through the liquid film (3×10^{-10} sec). It appears to be of the order of the exchange time in solid ^3He .⁴¹ This brings us again near the boundary between hydrogen and helium, where the liquid helium of the film is indeed compressed by the Van der Waals attraction of the solid hydrogen substrate, and may be solid or nearly so.

6. CONCLUSIONS

^4He films are effective coatings for preventing relaxation of polarized ^3He gases. We have shown that relaxation takes place inside the ^4He film, near the substrate boundary. The energy of ^3He in that region, deduced from a phenomenological model, was found to be of the order of 0.3 K, and in some samples -1.7 K.

Extrapolation to temperatures lower than 0.5 K suggests that the relaxation time would remain larger than 500 sec down to 0.3 K, unless ^3He - ^4He interaction in the adsorbed phase starts to become predominant, which remains to be investigated. Indirect evidence of a limited growth of solid hydrogen on glass has also been obtained.

ACKNOWLEDGMENT

The authors are very grateful to Professor J. Brossel for his constant interest in this work, to which he contributed much.

REFERENCES

1. M. Himbert, V. Lefevre-Seguin, P.-J. Nacher, J. Dupont-Roc, M. Leduc, and F. Laloë, *J. Phys. Lett. (Paris)* **44**, L-523 (1983).
2. R. Barbé, M. Leduc, and F. Laloë, *Phys. Rev. Lett.* **34**, 1488 (1975).
3. R. Chapman and M. Bloom, *Can. J. Phys.* **54**, 861, 1831 (1976).
4. V. Lefevre-Seguin, P.-J. Nacher, J. Brossel, W. N. Hardy, and F. Laloë, *J. Phys. (Paris)* **46**, 1145 (1985).
5. V. Lefevre-Seguin, unpublished Thèse de doctorat d'état, Université Paris VI (1984).
6. P. Seligman, D. O. Edwards, R. E. Sarwinski, and J. T. Tough, *Phys. Rev.* **181**, 415 (1969).
7. C. Ebner and D. O. Edwards, *Phys. Reports* **2**, 77 (1970).
8. I. F. Silvera and J. T. M. Walraven, *Phys. Rev. Lett.* **45**, 1268 (1980).
9. M. Morrow, R. J. Jochemsen, A. J. Berlinsky, and W. N. Hardy, *Phys. Rev. Lett.* **46**, 195; **47**, 852 (1981).
10. R. W. Cline, T. J. Greytak, and D. Kleppner, *Phys. Rev. Lett.* **47**, 1195 (1981).
11. M. G. Richards *J. Phys. (Paris)* **39**, C6-1342 (1978); H. Godfrin, G. Frossati, D. Thoulouze, and M. Chapellier, *J. Phys. (Paris)* **39**, C6-287 (1978).
12. R. G. Richardson, *Physica B + C* **126**, 298 (1984), and references therein.

13. A. Taber, *J. Phys. (Paris)* **39**, C6-192 (1978).
14. P.-J. Nacher, G. Tastevin, M. Leduc, S. B. Crampton and F. Laloë, *J. Phys. Lett. (Paris)* **45**, L-441 (1984).
15. M. Leduc, P.-J. Nacher, D. S. Betts, J. M. Daniels, G. Tastevin and F. Laloë, *Europhys. Lett.* **4**, 59 (1987).
16. G. Tastevin, P.-J. Nacher, L. Wiesenfeld, M. Leduc and F. Laloë, *J. Phys. (Paris)* **49**, 1 (1988).
17. F. M. Ellis and R. B. Hallock, *Phys. Rev. B* **29**, 497 (1984); J. M. Valles Jr., R. H. Highley, R. B. Johnson and R. B. Hallock, *Phys. Rev. Lett.* **60**, 428 (1988).
18. J. P. Laheurte, J. C. Noiray, J. P. Romagnan and D. Sornette, *J. Phys. (Paris)* **47**, 39 (1986).
19. B. K. Bhattacharyya and F. M. Gasparini, *Phys. Rev. Lett.* **49**, 919 (1982).
20. D. S. Sherril and D. O. Edwards, *Phys. Rev. B* **31**, 1338 (1985).
21. C. P. Lusher, M. F. Secca and M. G. Richards, *J. Low Temp. Phys.* **72**, 71 (1988).
22. C. P. Lusher, unpublished Ph.D. Thesis, The University of Sussex, Brighton (1985).
23. G. Tréneç, P.-J. Nacher and M. Leduc, *Opt. Commun.* **43**, 37 (1982).
24. P.-J. Nacher and M. Leduc, *J. Phys. (Paris)* **46**, 2057 (1985).
25. A. Abragam, *Principles of Nuclear Magnetism* (Oxford University Press, Oxford, 1961).
26. L. D. Schearer and G. K. Walters, *Phys. Rev.* **139A**, 1398 (1965); V. Lefevre, P. J. Nacher, F. Laloë, *J. Phys. (Paris)* **43**, 89 (1982).
27. B. Shizgal, *J. Chem. Phys.* **58**, 3424 (1973); *Can. J. Phys.* **54**, 164 (1976).
28. J. Wilks, *The Properties of Liquid and Solid Helium* (Oxford University Press, Oxford, 1967).
29. D. Cieslikowski, A. S. Dahm and P. Leiderer, *Phys. Rev. Lett.* **58**, 1751 (1987); M. A. Paalanen and Y. Iye, *Phys. Rev. Lett.* **55**, 1761 (1985).
30. J. Frenkel, *Kinetic Theory of Liquids* (Oxford University Press, Oxford, 1946); G. D. Halsey, Jr., *J. Am. Chem. Soc.* **73**, 2693 (1951); T. L. Hill, *J. Chem. Phys.* **17**, 500 (1948); I. E. Dzyaloskinskii, E. M. Lifshitz and L. P. Pitaevskii, *Adv. Phys.* **10**, 165 (1961).
31. M. Himbert, J. Dupont-Roc and C. Lhuillier, *Phys. Rev. A* (1989, to be published).
32. J. G. Dash, *Films on Solid Surfaces* (Academic Press, New York, 1975).
33. J. Krim, J. G. Dash and J. Suzanne, *Phys. Rev. Lett.* **52**, 641 (1984).
34. A. D. Migone, J. Krim, J. G. Dash, and J. Suzanne, *Phys. Rev. B* **31**, 7643 (1985); P. Taborek, L. Senator, *Phys. Rev. Lett.* **57**, 218 (1986).
35. K. Takahashi, *Faraday Trans. 1* **78**, 2059 (1982).
36. H. K. Pulker, *Coatings on Glass*, (Elsevier, New York, 1985), Sec. 3.1.5.
37. M. A. Bouchiat and J. Brossel, *Phys. Rev.* **147**, 41 (1966).
38. R. Chapman and M. Bloom, *Can. J. Phys.* **54**, 861 (1976).
39. A. J. Berlinsky, W. N. Hardy and B. W. Statt, *Phys. Rev. B* **35**, 4831 (1987).
40. M. Himbert, unpublished Thèse de Doctorat d'état, Université Paris VI (1987).
41. M. Roger, J. H. Hetherington and J. M. Delrieu, *Rev. Mod. Phys.* **55**, 1 (1983).